Influence of the Counterion on the Local Environment and Electronic Structure of Active Sites in Zeotypes

Furio Corà* and C. Richard A. Catlow

Davy Faraday Research Laboratory, The Royal Institution of Great Britain, 21 Albemarle Street, London W1S 4BS, U.K.

Received: June 3, 2003; In Final Form: July 24, 2003

We investigate, using periodic quantum mechanical calculations, how different counterions affect the geometrical and electronic structure of Al^{3+} and Fe^{3+} active sites in zeolites and AlPOs. Association of the counterion with one or more framework oxygens modifies their bond lengths within the framework, including the distance from the dopant ion, and hence the symmetry of the active sites. The average bond length of the dopant with its four oxygen neighbors is, however, only marginally affected by the type of counterion. We further find that the presence of framework dopants influences the electronic structure, and in particular that low-valent dopant ions are ionic, while causing an increase of covalence in the surrounding region of the framework.

1. Introduction

The microporous nature of the crystalline framework in zeotype materials, such as aluminophosphates (AlPOs) and silica-based zeolites, enables an effective size- and shape-selective control at the molecular level of the processes that occur within the structure, and makes these materials of interest for heterogeneous catalysis.[1,2] The catalytic activity in zeotypes is associated with the presence of framework defects; the type and number of active sites can be controlled during the synthesis by appropriate chemical doping, via the isomorphous substitution of heteroatoms in the framework. Apart from seeding the catalytic activity, the presence of low-valence framework ions is also required to provide charge-balance for the positive charge of the cationic template molecules,[3] used in the synthesis of zeotypes as structure-directing agents to yield the microporous framework architecture.

After the zeotype framework is obtained, its chemical composition can be modified in postsynthetic treatments: calcination of the as-synthesized material, for instance, is required to remove the organic template molecules and activate the catalytic behavior of the solid. During the calcination, low-valence ions can be oxidized to isovalent, yielding a charge-neutral framework structure, which is the case for redox-active dopant ions, such as Fe^{2+} in Fe-doped AlPOs, which is oxidized to the 3+ state.[4] When the charge of the low-valence ions is retained in the calcination, instead, upon removal of the organic template the structure requires the presence of extraframework cations to preserve its charge neutrality. In the latter case, the organic cationic template is replaced during the calcination by an acid proton bonded to one of the framework oxygen atoms, resulting in the creation of Brønsted acid sites. The type of charge-balancing cation can be further modified by ion-exchange operations, and the proton replaced by larger inorganic cations, such as Na^+, K^+, or polyvalent ions. Calcination in the presence of non redox-active ions can also be viewed as a special case of cation exchange, in which the organic template is replaced by a proton.

The crystalline environment of the active sites is modified during these postsynthetic operations, which may influence the structural and electronic properties of the dopant ions, and hence also the catalytic activity. We know in fact that the catalytic properties of doped zeotypes are primarily dependent upon the *type* of metal dopant employed,[5] but the constrained environment in which the active site is hosted in the microporous framework contributes to defining the catalytic activity of the material. Understanding the structural and electronic properties associated with dopant ions in zeolites and AlPOs, and how the chemistry of the dopants is influenced by the crystalline environment, including the counterion, is therefore a step of crucial importance in controlling the catalytic activity and selectivity of these heterogeneous catalysts.

Experimentally, the local environment of the dopant ions, and the location of the counterions, can be investigated by diffraction methods only if the inclusion of the dopant in the framework is long-range ordered, which is rarely the case, except at very high concentrations (see, e.g., refs 6,7). Low levels of doping usually result in a disordered incorporation of the dopants in the zeotypic framework. In this case, structural information on the dopants can be derived by means of element-specific techniques, such as X-ray absorption spectroscopy (XAS), and in particular EXAFS.[8] However, these techniques provide average values for the selected element over the whole material; when more than one coordination environment and/or oxidation state are present, the experimental result is a weighted average of all the local environmental structures in which the dopant ions are hosted (see, e.g., refs 4, 9, 10). For a proper characterization of the catalyst, it would be desirable to have means to investigate each local environment independently. When calcination to remove the organic template can oxidize, at least partially, the defect centers of the structure, one method to select the reduced oxidation state is to perform the experimental measurements on the as-synthesized form of the material.[11,12] Moreover, we can exploit the possibility of modifying the chemical composition of the solid via ion-exchange processes; for certain oxidation

* Corresponding author. Fax: +44-(0)20-76293569. E-mail: furio@ri.ac.uk.

10.1021/jp035552t CCC: $25.00
Published on Web 10/04/2003

states of the dopant ions, in fact, the ion-exchanged form of the material may be more stable than the catalytically active acid form, and hence be more suitable for experimental characterization. We may therefore wonder whether the information obtained on the as-synthesized or ion-exchanged material is relevant for the description of the active sites in the activated (calcined) catalyst, and how much the presence of different counterions affects the properties of the active sites.

Computer modeling techniques allow an easy control of the structural parameters listed above, such as the oxidation state of the active site and the composition of the material. We have therefore applied accurate quantum mechanical methods to investigate how different counterions affect the structure and chemistry of the active sites in zeotypes. In this paper, we describe the properties of two trivalent ions, namely Al^{3+} and Fe^{3+}, in the CHA framework type of the zeolite chabasite and its isostructural aluminophosphate, AlPO-34. In the zeolite framework, 3+ ions represent low-valence defect centers, which require charge compensation. The low-valent substitution of the Al^{3+} and Fe^{3+} ions for Si^{4+} in chabasite has been charge-balanced in our calculations by protonating one of the framework oxygens nearest neighbors of the dopant, or by adding one Li, Na, or K extraframework ion. It is also of interest to compare the local structure of the 3+ metal ions in zeolites with that in AlPOs, where the 3+ ions are isovalent (the host ion itself in the case of Al), and hence do not require charge compensation. It has been shown[13] that the Lewis acidity of the counterion scales as Q/R^2, where Q is the formal ionic charge (+1 in the cases examined here) and R the ionic radius. In this view, the noncounterion situation of AlPOs can be considered as equivalent to a counterion of charge +1 and of infinite size. The charge-balancing ions examined here span therefore the complete range of ionic sizes, from the smallest countercation (H), to extraframework ions of increasing size (Li, Na, K), to the noncounterion situation in AlPO-34. Examining the local structural environment of Al^{3+} and Fe^{3+} ions in chabasite and AlPO-34 enables us to investigate how much the presence and type of counterion can influence the structural and electronic properties of the dopant.

2. Computational Details

The doped framework of chabasite and AlPO-34 is described in our calculations under periodic boundary conditions, via a supercell model, in which one dopant ion is included in each unit cell of the host framework (composed of 36 atoms). Even at this relatively high concentration, the dopant ions are separated by ~10 Å from each other, and represent therefore noninteracting defect centers. The supercell model provides a correct description of the crystalline environment of the active site, including the crystal field and the structural strain caused by the crystalline matrix on the substitutional ion.

Since the Fe^{3+} dopants are open-shell transition metal ions, we performed our calculations at the Unrestricted Hartree−Fock (UHF) level; this Hamiltonian employs the exact expression of exchange forces, which are important for a correct representation of the unpaired electrons on the Fe^{3+} site. We used the latest version of the code CRYSTAL.[14]

For each combination of dopant and counterion investigated, we have performed a geometry optimization to determine the equilibrium structure. Analysis of the bonding properties of the dopant to the zeotype framework is performed on the equilibrium geometry.

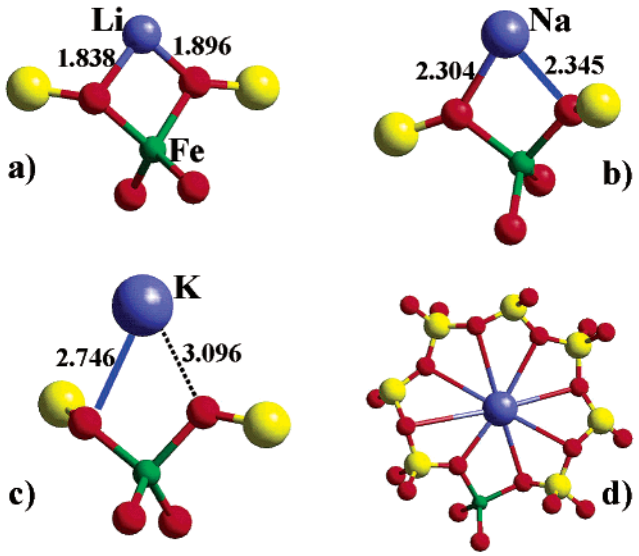

Figure 1. Equilibrium structure of (a) Li^+, (b) Na^+, and (c) K^+ counterions next to an Fe^{3+} substitutional dopant in chabasite. (d) Equilibrium position of the K^+ ion, highlighting its location near the center of one eight-membered ring of tetrahedra of the chabasite structure.

TABLE 1: Equilibrium Bond Distance(s) R_n, in Å, between the Counterions Examined and the Framework Oxygens, in Order of Increasing Bond Distance[a]

ion	H		Li		Na		K	
dopant	Al^{3+}	Fe^{3+}	Al^{3+}	Fe^{3+}	Al^{3+}	Fe^{3+}	Al^{3+}	Fe^{3+}
R_1	0.949*	0.948*	1.921*	1.838*	2.286*	2.304*	2.769*	2.746*
R_2			2.061*	1.896*	2.549	2.345*	3.064	3.096*
R_3			2.380		2.662	2.702	3.158*	3.189
R_4							3.171	3.198
R_5							3.299	3.255
R_6							3.361	3.297
R_7							3.509	3.427

[a] Numbers marked with the symbol * refer to the oxygen nearest neighbors of the dopant ion.

3. Results and Discussion

Results of the geometry optimizations are reported in Tables 1−3 for the counterion location, and the structural and electronic parameters of the dopant, respectively. In Figure 1, we also report a graphical representation of the equilibrium structure for the Fe^{3+} dopant in chabasite, with Li, Na, and K counterions.

3.1. Counterion Location. Let us first consider how the size of the counterion affects its interaction with the framework oxygens. In Table 1 we report the calculated bond distances in the equilibrium structure between each counterion examined and the framework oxygens, in order of increasing distance; the values marked with a symbol (*) refer to the oxygen atom nearest neighbors of the dopant.

We see in Table 1 that H has an obvious association with only one oxygen, the one to which it is covalently bonded to form the OH Brønsted acid site. Given the importance of acid zeolites in heterogeneous catalysis, the Al(OH) site in zeolites has been characterized with a variety of computational techniques, including isolated[15] and embedded[16−18] quantum mechanical (QM) clusters, supercell techniques,[19,23] and force field methods.[24] Taking into account the small difference in the calculated bond distances between these publications, dictated by the different framework topology and/or Al content in the solid examined, our results on the structure of the Al(OH) active site are in agreement with the computational literature, and the

TABLE 2: Equilibrium Bond Distances R_n, in Å, between the Dopant and Its Four Framework Oxygen Neighbors, in Order of Increasing Bond Distance[a]

	R_1	R_2	R_3	R_4	$\langle R \rangle$
Al^{3+}					
H	1.6787	1.6902	1.6974	1.8994*	1.7414
Li	1.6972	1.6988	1.7310*	1.7907*	1.7290
Na	1.6975	1.7066	1.7278	1.7672*	1.7248
K	1.6993	1.7182	1.7230	1.7486*	1.7223
AlPO	1.7195	1.7229	1.7287	1.7334	1.7261
Fe^{3+}					
H	1.8222	1.8282	1.8358	2.0660*	1.8880
Li	1.8270	1.8364	1.9024*	1.9367*	1.8756
Na	1.8314	1.8497	1.8744*	1.9161*	1.8679
K	1.8446	1.8651	1.8666	1.9011*	1.8693
FAPO	1.8649	1.8654	1.8678	1.8808	1.8697

[a] $\langle R \rangle$ indicates the average of the four bond distances R_{1-4}. Numbers marked with the symbol * refer to the oxygens closely associated with the counterion.

structure of the Brønsted acid site will not be discussed here. The equilibrium structure is instead different for the other extraframework ions, which have an ionic type of interaction with the framework oxygens. These ions are effectively "solvated" by the zeolitic framework, and show a marked association with two or more of the framework oxygens. The number of framework oxygens with which the extraframework ion is in close contact depends on the relative size of the ion itself and of the interstices available in the microporous zeotypic structure; in the same zeolite type, it increases on increasing the ionic size of the extraframework ion. We see, in Table 1 and Figure 1a, that the small Li^+ ions are located in a bridging position between two oxygens, both nearest neighbors of the Al or Fe dopant, with similar but unequal Li−O bond distances. The larger Na^+ ions, when located next to an Al dopant, increase their coordination number to the framework oxygens to 3, of which only one is nearest neighbor to the Al dopant. The shortest Na−O bond length, of 2.286 Å, is achieved with the latter oxygen, while the other two are ∼0.3 Å longer. The local structure of Na^+ calculated here, is similar to that of the ion labeled as Na5 in site III′ in the experimental work on the NaX zeolite.[7] When Na^+ is next to an Fe^{3+} dopant, which is larger than Al^{3+} (compare the Al−O and Fe−O bond distances in Table 2), the spacing between the oxygens nearest neighbors to Fe increases, and appears to be of optimal size to host the extraframework Na^+. The Na^+ ion in Fe-doped chabasite, therefore, has two short and one long bond distances with the framework oxygens. The even larger K^+ ions, finally, are located close to the center of eight-membered rings, where they can interact with up to eight framework oxygens. This increase in coordination number of K^+ is achieved partially by weakening its association with the framework oxygens that are nearest neighbor to the dopant (for both Al and Fe ions), with which K^+ retains only one short bond. If the stable local environment of K^+ in the eight-membered rings of the chabasite structure found here has general validity also for other framework types, we may expect the presence of K^+ ions to obstruct the eight-membered ring openings, and hence to hinder the diffusion of molecular species within the structure. Experimental studies are required to verify if this is indeed the case. When considering the effect of the extraframework ion on the dopant, it is important to note that the association of K^+ is appreciable with only one of the framework oxygens that are nearest neighbor to the dopant.

The location of extraframework Li, Na, and K ions has been investigated with quantum mechanical[25−27] and force field-based[28−30] computational methods in other zeolitic framework types, all of which have different pore openings from the chabasite polymorph examined here. The trend relative to the increase of coordination number of the extraframework ion with its ionic size, found here in chabasite, is common to the offretite[25] and faujasite (X)[27] zeolitic structures, and can therefore be assumed to have general validity. The organic template molecules employed in the synthesis of zeotypes have even larger size than the K^+ ion examined here and, especially when they have high symmetry, we expect them to behave in a similar way to K^+, i.e., with a weak association with several framework oxygens, not necessarily nearest neighbors of the dopant ion.

From a computational point of view, it is of interest to examine the symmetry of the extraframework ion position calculated with different models of the active site. QM studies performed with models of the solid based on periodic boundary conditions,[25,26,28] such as the one employed here, yield equilibrium structures in which the bond distances between the extraframework ion and framework oxygens are different from each other; the same result is obtained experimentally.[7] Models of the active site based on isolated cluster techniques, instead, tend to favor a structure in which the local environment of the extraframework ion is much more symmetric, with distances from the framework oxygens more similar (or equal) to each other (see for instance ref 27). We consider that the latter result highlights a limitation of cluster model studies; if not accurately chosen, the molecular fragment employed to represent the zeolitic framework is under-constrained, and it can adapt too easily around the extraframework cation, thus yielding an equilibrium structure in which the distance of each framework oxygen from the extraframework cation is individually optimized (and thus equal). This is not the case in the true (extended) solid, where the equilibrium location of the extraframework ion is due to a compromise between the highest coordination number and the strength of its interaction with each framework oxygen. Periodic studies, based on a supercell-model description of the dopant ion, reproduce correctly this behavior, even when the dopant concentration in the framework is high, as in the present work.

3.2. Framework Structure. Our calculations suggest not only that the framework structure and composition influence the location of extraframework ions, but also that the opposite process is important, i.e., that the type and location of the extraframework ion can modify the framework properties. In the following discussion we shall examine how the type, and especially the location, of the counterion in the structure influences the properties of the framework oxygens and of the dopant ions (M), both structural (Table 2) and electronic (Table 3). By analyzing the data of Table 2, we find that those O ion-(s) that are in closer contact with the counterion (marked with a symbol (*) in Tables 2 and 3) have M−O bonds that are sizeably longer than those of the oxygens not closely associated to the counterion. This feature of the counterion, i.e., the number of oxygens with which it is in close contact, can therefore make a substantial difference in determining the local structural environment of the dopant.

We see in Table 2 that the influence of the counterion on the framework oxygens scales inversely with the size of the counterion. The Al−O(H) bond length of the dopant Al with the protonated oxygen in chabasite is 0.210 Å longer than (the average of) the other 3 Al−O distances. The difference (Δd) in the Al−O bond distance of the Al dopant with the oxygen(s) associated and not with the counterion decreases to 0.082, 0.057, and 0.035 Å for the Li, Na, and K counterions, respectively.

TABLE 3: Electronic Distribution, Measured via a Mulliken Population Analysis, of the Al^{3+} and Fe^{3+} Dopant Ions in Chabasite and AlPO-34 as a Function of the Counterion[a]

	Q_M	Q_{b1}	Q_{b2}	Q_{b3}	Q_{b4}	Q_{T4}	Q'_{b4}	Q_{T1}	Q'_{b1}
Al^{3+}									
H	2.113	.178	.171	.173	.076*	2.035	.183	2.006	.360
Li	2.119	.165	.161	.153*	.118*	1.971	.311	2.001	.377
Na	2.118	.164	.155	.152	.127*	1.977	.333	1.997	.379
K	2.114	.162	.148	.153	.137*	2.030	.350	1.997	.380
AlPO	2.191	.139	.139	.139	.136				
Fe^{3+}									
H	2.146	.135	.123	.127	.050*	2.029	.197	2.017	.366
Li	2.131	.132	.125	.096*	.091*	1.986	.318	2.011	.371
Na	2.131	.125	.119	.101*	.097*	1.987	.341	2.007	.380
K	2.134	.124	.107	.114	.100*	1.978	.356	2.011	.384
FAPO	2.230	.100	.100	.099	.099				

[a] The symbols used are illustrated in Figure 3a, and refer to: net charge of the dopant (Q_M); bond population of the dopant with the four oxygen neighbors Q_{bn}; bond population of the oxygens O_1 and O_4 (those with the shortest and longest M−O distance) with their neighbor Si ion of the host framework in chabasite (Q'_{bn}), and net charge (Q_{Tn}) of these two Si ions. Charges are measured in |e|. The values marked with a * refer to the oxygens in close association with the counterion. The corresponding values of Q_T and Q'_b in undoped chabasite are 2.03 and 0.29 |e|.

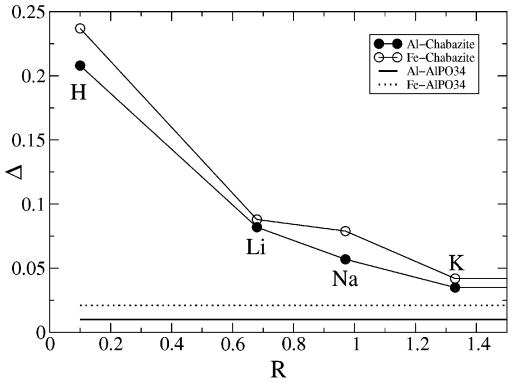

Figure 2. Effect of different counterions on the structure of the dopant in chabasite and AlPO-34. Δd is the structural anisotropy in the coordination environment of the dopant, defined in the text; R is the ionic size of the counterion, in Å. Filled and empty symbols refer to the Al^{3+} and Fe^{3+} dopant ions, respectively.

The same values are of 0.237, 0.088, 0.079, and 0.042 Å for the Fe dopant, charge balanced with H, Li, Na, and K ions, respectively. The structural anisotropy around the dopant with the K^+ counterion is similar to the noncounterion situation seen in AlPO-34, where the difference between the longest M−O bond and the average of the other three is 0.010 Å for Al and 0.021 Å for Fe^{3+}. We can therefore consider this structural parameter calculated for K^+ as being nearly converged as a function of the counterion size, and we expect extraframework cations larger than K^+, including the organic templates, not to introduce substantial structural differences around the dopant. If we take the parameter Δd as being representative of the effect of the extraframework ion on the structure of the dopant (active site) in the framework, and plot Δd as a function of the ionic size R (see Figure 2), the correlation between the ion type and the structural distortion it introduces in the framework becomes evident: the smaller the size of the extraframework ion, the larger its effect on the framework structure. This result is in agreement with the strength of Lewis acidity of the extraframework ion, QR^{-2} proposed in reference 13; however, the different coordination environment of each counterion examined makes the validity of the R^{-2} dependence of Δd on R only approximate.

For the experimental characterization of catalysts, it is of

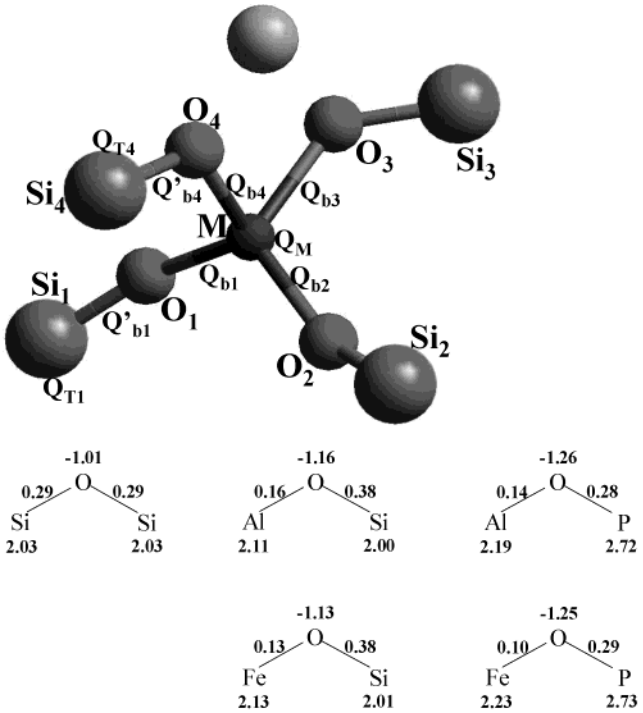

Figure 3. (a) Explanation of the symbols used in Table 3; (b) electronic distribution, measured via a Mulliken population analysis, of the framework ions in pure and doped chabasite and AlPO-34. The values refer to net atomic charges and bond populations, measured in |e|.

interest to notice that the association of the counterion with one or more of the framework oxygens alters substantially the individual M−O bond distances in the framework, and hence also the local symmetry around the dopant M, but not the value of the M−O distance averaged over the 4 M−O bonds of its tetrahedral environment. Moreover, for both Al^{3+} and Fe^{3+} ions, the average M−O bond distance in AlPO-34 is very similar to that in chabasite (within the experimental error of ±0.02 Å in bond distances associated with EXAFS techniques), and is therefore dictated only by the ionic radius of the dopant, and not by its crystalline environment. Our results suggest therefore that the experimental values of the bond distances obtained from EXAFS data, expecially when they are fitted using 4 M−O bonds of the same length (as is often the case), are transferable from one counterion to the others, and the results obtained for the as-synthesized or cation-exchanged form apply also to describe the dopant ions in the activated catalyst.

3.3. Electronic Distribution. The effects of the counterion are pronounced not only on the equilibrium M−O distances, but also on the bonding character of the dopant to the framework ions. Results analyzing this feature are summarized in Table 3 and Figure 3, where we report the Mulliken net charge of the dopant (Q_M), and its bond population with the four oxygen neighbors Q_{bn}. We also report the bond population Q'_{bn} of the oxygens O_1 and O_4 (those with the shortest and longest M−O distance) with their neighbor Si ion of the host framework in chabasite, and the net charge (Q_T) of these two Si ions. The values of the net and bond charges reported in Table 3 enable us to understand the chemistry of the dopant and framework ions, and in particular to investigate the covalent/ionic picture of Fe−O and Al−O bonds in the solid as a function of the local environment and counterion. The results of our calculations indicate that when the oxygen ions of the framework are located between two cations of different formal charges, they form a covalent bond with the neighbor with higher charge, and an ionic bond with the neighbor with lower charge. The larger the

difference in charge between the two T sites bonded to the same oxygen, the larger the difference in the nature of the two T−O bonds. We have shown in previous publications that in pure AlPOs the P−O bonds are covalent, while the Al−O bonds are ionic.[31,32] The framework oxygens next to the undervalent dopant in chabasite are bonded to one 3+ and one 4+ atoms; they react to this charge inequivalence of their two neighbors by bonding more covalently to the framework Si. The Si−O bond population increases from 0.29 |e| in the undoped chabasite framework to ∼0.38 |e| for the Si atom bonded to O_1. At the same time, the net charge of the silicons that are next-nearest neighbor to the 3+ dopant decreases, confirming a more covalent nature of their bonding with the oxygens. If we further consider the bonding of the dopant with its nearest oxygens, we see that both Al and Fe have higher values of Q_b in the zeolite framework than in AlPOs (the difference being of ∼0.03 |e| in the bond to each oxygen that is not associated with the extraframework ions). As a result, the net positive charge of the dopant is higher in AlPO-34 than in chabasite. The above comparisons indicate that the oxygens in the framework are more polarized toward P in AlPOs than toward Si in chabasite. Our calculations show therefore that low valent dopants are ionic, and increase the covalence of the framework in the neighboring region. We expect this feature to influence the chemical and catalytic behavior of the dopant; in particular, the Lewis acidity of the dopant is linked to the ionicity of the M−O bonds. Ionic bonds are nondirectional, and provide a more flexible coordination environment for the dopant ion toward changes of its coordination number in the presence of Lewis bases. From the results of our calculations, we expect therefore a more pronounced Lewis acid behavior of the same dopant ion in AlPOs than in zeolites, which is another prediction of this computational work that we leave open for future experimental studies.

4. Conclusions

In summary, we have examined the effect of different extraframework ions on the structural and electronic properties of Al^{3+} and Fe^{3+} dopant ions in the chabasite framework of zeolites and AlPOs. The association of the extraframework ions with the framework oxygens is most effective for small ions, while the number of framework oxygens in close contact with the counterion increases with the ionic size of the latter. The extraframework ion modifies the bond lengths and electronic distribution of the dopant, but not the value of the bond length averaged over the four nearest oxygens, which can therefore be transferred across different extraframework ions, including the organic template molecules employed in the synthesis of zeotypes. Analysis of the electronic distribution in isostructural zeolites and AlPOs suggests a more ionic nature of dopants in the AlPO framework, from which we expect doped AlPOs to have more pronounced Lewis acidity properties than zeolites.

Acknowledgment. We thank EPSRC for funding this research project, and acknowledge a grant to F.C. from the Royal Society for the purchase of computer equipment.

References and Notes

(1) Corma, A.; García, H. *Catal. Today* **1997**, *38*, 257.
(2) Thomas, J. M. *Angew. Chem., Int. Ed.* **1999**, *38*, 3589.
(3) Lewis, D. W.; Catlow, C. R. A.; Thomas, J. M. *Chem. Mater*. **1996**, *8*, 1112.
(4) Zenonos, C.; Sankar, G.; Corà, F.; Lewis, D. W.; Pankhurst, Q. A.; Catlow, C. R. A.; Thomas, J. M. *Phys. Chem. Chem. Phys.* **2002**, *4*, 5421.
(5) Hočevar, S.; Batista, J.; Kaučič, V. *J. Catal.* **1993**, *139*, 351.
(6) Mortier, W. J. *Compilation of Extraframework Sites in Zeolites*; Butterworth-Heinemann: London, 1982.
(7) Olson, D. H. *Zeolites* **1995**, *15*, 439.
(8) Sankar, G.; Thomas, J. M.; Catlow, C. R. A. *Top. Catal.* **2000**, *10*, 255.
(9) Barrett, P. A.; Sankar, G.; Catlow, C. R. A.; Thomas, J. M. *J. Phys. Chem.* **1996**, *100*, 8977.
(10) Corà, F.; Sankar, G.; Catlow, C. R. A.; Thomas, J. M. *Chem. Commun.* **2002**, 734.
(11) Brückner, A.; Lohse, U.; Mehner, H. *Microporous Mesoporous Mater.* **1998**, *20*, 207.
(12) Sankar, G.; Thomas, J. M.; Chen, J.; Wright, P. A.; Barrett, P. A.; Greaves, G. N.; Catlow, C. R. A. *Nucl. Instrum. Methods Phys. Res.* B **1995**, *97*, 37.
(13) Huang, M.; Kaliaguine, S. *Stud. Surf. Sci. Catal.* **1993**, *78*, 559.
(14) Saunders, V. R.; Dovesi, R.; Roetti, C.; Orlando, R.; Zicovich-Wilson, C. M.; Harrison, N. M.; Doll, K.; Civalleri, B.; Bush, I.; D'Arco, Ph.; Llunell, M. *CRYSTAL2003 User's Manual*; University of Torino: Torino, 2003.
(15) Sauer, J. *Chem. Rev.* **1989**, *89*, 199; Sauer, J. In *Modelling of structure and reactivity in Zeolites*; Catlow, C. R. A., Ed.; Academic Press: London, 1992; p 183.
(16) Brändle, M.; Sauer, J. *J. Am. Chem. Soc.* **1998**, *120*, 1556.
(17) Sierka, M.; Sauer, J. *Faraday Discuss.* **1997**, *106*, 41.
(18) Treesukol, P.; Lewis, J. P.; Limtrakul, J.; Truong, T. N. *Chem. Phys. Lett.* **2001**, *350*, 128.
(19) Haase, F.; Sauer, J. *J. Am. Chem. Soc.* **1995**, *117*, 3780.
(20) Ugliengo, P.; Civalleri, B.; Zicovich-Wilson, C. M.; Dovesi, R. *Chem. Phys. Lett.* **2000**, *318*, 247.
(21) Shah, R.; Gale, J. D.; Payne, M. C. *Chem. Commun.* **1997**, 131.
(22) Shah, R.; Gale, J. D.; Payne, M. C. *Phase Transitions* **1997**, *61*, 67.
(23) Jeanvoine, J.; Ángyán, J. G.; Kresse, G.; Hafner, J. *J. Phys. Chem. B* **1998**, *102*, 5573.
(24) Jackson, R. A.; Catlow, C. R. A. *Mol. Simul.* **1988**, *1*, 207.
(25) Campana, L.; Selloni, A.; Weber, J.; Goursot, A. *J. Phys. Chem. B* **1997**, *101*, 9932.
(26) Goursot, A.; Vasilyev, V.; Arbuznikov, A. *J. Phys. Chem. B* **1997**, *101*, 6420.
(27) Deka, R. Ch.; Hirao, K. *J. Mol. Catal. A* **2002**, *181*, 275.
(28) Mellot-Draznieks, C.; Buttefey, S.; Boutin, A.; Fuchs, A. H. *Chem. Commun.* **2001**, 2200.
(29) Newsam, J. M.; Freeman, C. M.; Gorman, A. M.; Vessal, B. *Chem. Commun.* **1996**, 1945.
(30) Ruiz-Salvador, A. R.; Lewis, D. W.; Rubayo-Soneira, J.; Rodriguez-Fuentes, G. *J. Phys. Chem B* **1998**, *102*, 8417.
(31) Corà, F.; Catlow, C. R. A. *J. Phys. Chem. B* **2001**, *105*, 10278.
(32) Corà, F.; Catlow, C. R. A.; D'Ercole, A. *J. Mol. Catal. A: Chem.* **2001**, *166*, 87.